Available online at www.sciencedirect.com
SCIENCE DIRECT®
International Journal of Heat and Mass Transfer 47 (2004) 1561–1567
International Journal of HEAT and MASS TRANSFER
www.elsevier.com/locate/ijhmt

Technical Note

Laminar mixing induced by a twisted quadripolar Stokes flow

J.P. Brancher *, J.C. Leprevost

LEMTA, 2 avenue de la forêt de Haye, 54504 Vandoeuvre les Nancy, France

Received 12 March 2002

Abstract

The aim of this paper is to study the laminar mixing induced by a quadripolar Stokes flow superimposed to an axial Poiseuille flow. When the two-dimensional quadripolar flow is twisted along the direction of the Poiseuille flow, advection becomes chaotic. This three-dimensional open flow device is applied to the mixing of a dye injected continuously on a fraction of the entrance section.

Keywords: Chaotic advection; Laminar mixing; Magnetohydrodynamics

1. Introduction

It is well known that chaotic mixing in two-dimensional Stokes flows occurs in the annular region between two eccentric periodically rotating circular cylinders [1–4]. Also, the flow obtained between two confocal ellipses, which circumferences are periodically rotating, leads to an interesting chaotic mixing pattern [5]. In general, the superposition of an axial laminar flow to one of the above two-dimensional flows generates a three-dimensional open flow mixing device. Brancher and Goichot [6] recently pointed out that chaotic advection can occur when a circular quadrupole plane flow is periodically rotated around its centre. Such a flow is obtained in a cylindrical cavity, filled with an electrical conducting fluid, and submitted to the magnetic field created by two coils rotating periodically and slowly around the cylinder. For high current frequencies and small Reynolds and Stokes numbers, the velocity field can be calculated analytically. The Stokes number represents the ratio between the typical time scale of the flow and the typical time scale of the coils oscillations. So, if this Stokes number is very small, the quasi-steady approximation can be used. The advection properties of this two-dimensional unsteady flow have been studied in [7]. As stated earlier, when an axial laminar Poiseuille flow is superposed to the quadripolar flow, a steady three-dimensional mixing device is obtained. The same method can be used with eccentric cylinders or confocal ellipses [8,9], but the corresponding flows called "Eccentric helical annular flows" are time periodic rather than spatially periodic. Several papers proposed in the literature concern three-dimensional steady flows exhibiting chaotic advection: ABC flows [10]; bounded flows in spheres [11]; more recently, bounded flows obtained with orthogonal vortices [12]. The present case is connected with steady open flows such as the twisted pipe case [13,14] and the "partitioned pipe mixer" [8]. These flows are spatially periodic, the presence of vortices in the orthogonal plane of the axis of the duct playing a fundamental role in the mixing. The present open flow is obtained first by twisting a quadripolar two-dimensional velocity field along the z-axis. The two-dimensional basic flow $\vec{u}(r,\theta)$ which analytic expression is briefly developed in the appendix, has been established in [6]. This flow takes place in a cylinder of radius R_0 with a typical velocity u_0 and the streamlines are shown on Fig. 1a. The three-dimensional open flow (Fig. 1b) results from the superposition of an axial creeping flow to the previous two-dimensional flow and can be expressed by:

$$\vec{V} = \vec{u}(r,\theta-\varphi(z)) + W(r)\vec{e}_z \tag{1}$$

* Corresponding author.
E-mail address: brancher@ensem.inpl-nancy.fr (J.P. Brancher).

0017-9310/$ - see front matter © 2003 Elsevier Ltd. All rights reserved.
doi:10.1016/j.ijheatmasstransfer.2003.03.003

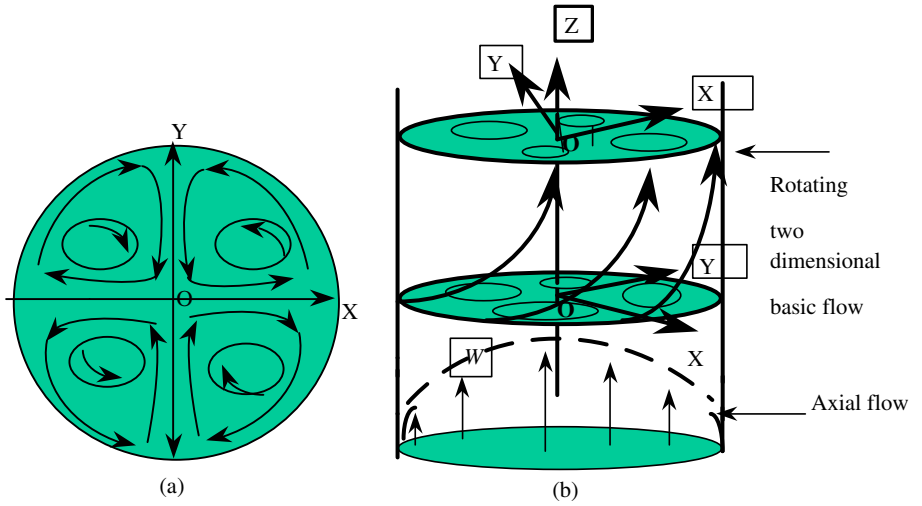

Fig. 1. (a) Two-dimensional basic flow. (b) Three-dimensional open flow.

where r, θ, z are the cylindrical co-ordinates, $W(r)\vec{e}_z$ is the Poiseuille axial velocity in the circular cylinder: $W = 2W_0(1-r^2)$, W_0 is the mean velocity, $\vec{u}$ is the orthogonal plane flow, and φ is a periodic function of z.

First, we will look at the kinematic aspect and the Lagrangian trajectories of this flow. Then, the mass and heat transfer efficiencies of this flow are considered using a Eulerian approach.

2. Chaotic advection

The following flow is considered (1): $\vec{V} = \vec{u}(r, \theta - \varphi(z)) + W\vec{e}_z$.

The typical tangent and axial flow velocities (u_0 and W_0) are assumed to satisfy:

$$\frac{u_0 R_0}{\nu} \ll 1 \quad \text{and} \quad \frac{W_0 R_0}{\nu} \ll 1 \tag{2}$$

φ is chosen to be a linear function of z on both half periods of the modulation (Fig. 2), with an amplitude $\varphi_m = 2\pi k$, where k is the rotation number.

The wavelength L_0 is such that: $\frac{L_0}{W_0} = 0\left(\frac{R_0}{u_0}\right)$.

So, the characteristic time of the change of plane configuration seen by a particle moving on the z-axis is the same as the typical time of the plane flow. Or when a particle moves on the z-axis, it encounters configuration changes at a time scale which is the flow time scale. The chaotic behaviour of the present flow derives from the behaviour of the two-dimensional basic flow and is obtained by periodic rotation of the quadripole along the z-axis [6].

This flow is obtained for an electrical conducting liquid in arranging a pair of coils with the geometry given by Fig. 3.

When $\frac{\varphi_m R_0}{L_0} = \frac{2\pi k R_0}{L_0} \ll 1$, the three-dimensional effect of the magnetic field can be neglected, and the two-dimensional flow on a horizontal section can be calculated using the result of [6].

This problem can be reduced to a non-linear stationary Hamiltonian two-dimensional problem. This result mentioned by Raynal [15] can be established with the following change of variables.

$$\begin{aligned} X &= x \\ Y &= \int_0^y W(x,\eta)\,\mathrm{d}\eta \\ H(X,Y,z) &= \psi(x,y,z) \end{aligned} \tag{3}$$

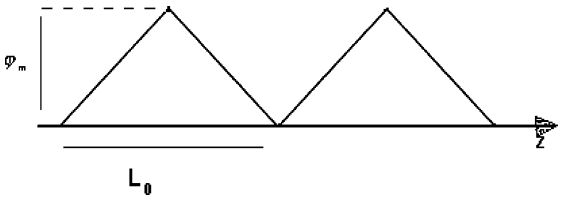

Fig. 2. Periodic rotation.

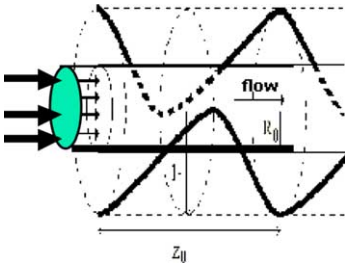

Fig. 3. Configuration of the coils.

Then

$$\frac{\partial X}{\partial z} = \frac{\partial H}{\partial Y}$$
$$\frac{\partial Y}{\partial z} = -\frac{\partial H}{\partial X} \quad (4)$$

The previous system is Hamiltonian but non-autonomous ($\frac{\partial H}{\partial z} \neq 0$).

We underline that the infinitesimal area $\mathrm{d}X\,\mathrm{d}Y = W\,\mathrm{d}x\,\mathrm{d}y$ represents the volumic flux.

The trajectories on Fig. 4 were obtained by numerical integration of $\frac{\mathrm{d}\underset{\sim}{x}}{\mathrm{d}t} = \vec{V}(\underset{\sim}{x})$.

3. Simple dynamic system

When the coils are far enough from the cylinder, only the leading term of the expression given in the appendix $\frac{\psi}{\psi_0} = r^2(1-r^2)\sin 2\theta$ is meaningful. ψ_0 is proportional to d^{-2}, where d is the distance from the coils to the z-axis.

For large values of d, the dimensionless form of the flow is reduced to the following analytic expression:

$$\vec{V} = \overrightarrow{\mathrm{rot}}[r^2(l-r^2)\sin 2(\theta-\varphi(z)]\vec{e}_z + 2a(1-r^2)\vec{e}_z \quad (5)$$

where

$$a = \frac{W_0}{u_0}, \quad \frac{\partial}{\partial z}\varphi(z) = \pm b$$
$$\text{for } z \in [0, L_0/2r_0] \text{ or } [L_0/2r_0, L_0/r_0]$$

and $b = \frac{2r_0\varphi_m}{L_0}$.

One can consider the formal non-dimensional 2D flow: $\psi = f(r)\sin n\theta$, with: $f(1) = 0$. For instance we can choose: $f(r) = (1-r^2)r$ and $n = 1$ corresponding to a dipolar Stokes flow. If this field rotates of $\varphi(t)$ with the period T, the trajectories are given by:

$$\frac{\mathrm{d}r}{\mathrm{d}t} = n\frac{f(r)}{r}\cos(n\alpha)$$
$$\frac{\mathrm{d}\alpha}{\mathrm{d}t} = -\frac{f'}{r}\sin(n\alpha) - \varphi'(t)$$

where $f' = \frac{\mathrm{d}f}{\mathrm{d}r}$, $\varphi' = \frac{\mathrm{d}\varphi}{\mathrm{d}t}$, and $\alpha = \theta - \varphi(t)$.

If φ is a triangular function: $\varphi' = +2\frac{\varphi_m}{T}$ on $[0, T/2]$ and $\varphi' = -2\frac{\varphi_m}{T}$ on $[T/2, T]$. This system depends on the three parameters: φ_m, T and n.

The 3D open flow will be given by:

$$\frac{\mathrm{d}r}{\mathrm{d}t} = n\frac{f(r)}{r}\cos(n\alpha)$$
$$\frac{\mathrm{d}\alpha}{\mathrm{d}t} = -\frac{f'}{r}\sin(n\alpha) \pm 2\frac{\varphi_m}{T}b(1-r^2)$$
$$\frac{\mathrm{d}z}{\mathrm{d}t} = b(1-r^2)$$

This system depends on the four parameters: b, φ_m, T and n.

4. Mass transfer problem

4.1. Presentation

In this section, the problem of a dye injection performed on a fraction of the entrance section is considered. At the boundary of the cylinder, there are no mass fluxes. The concentration distribution c of the colorant in a section S, situated n wavelengths after the entrance, is studied. The advection–diffusion of the dye concentration is solved.

Results obtained for different values of the Péclet number ($Pe = \frac{W_0 R_0}{D}$ where D is the dye diffusivity in the initial liquid) and for $\vec{u} = 0$, $\varphi = 0$ and $\varphi \neq 0$ are compared.

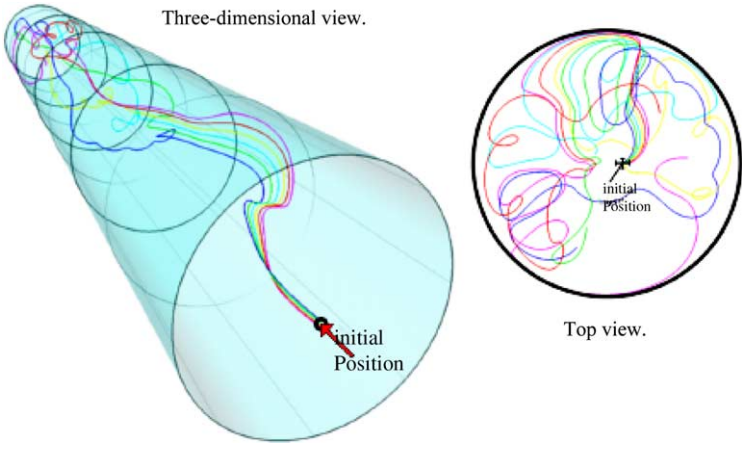

Fig. 4. Trajectories.

Three numbers calculated on the section ($r \leqslant 1$, $0 \leqslant \theta \leqslant 2\pi$, $z = nL_0$) can be used to characterize the mixture:

(a) The mean square concentration

$$\mu = \sqrt{\frac{1}{\pi R_0^2 W_0} \int W \cdot (c - \bar{c})^2 \, \mathrm{d}s} \tag{6}$$

where

$$\bar{c} = \frac{1}{\pi R_0^2 W_0} \int W \cdot c \, \mathrm{d}s \tag{7}$$

(b) The contaminated surface ratio

$$S_e = -\frac{1}{\pi R_0^2} \int H(c - \bar{c}) \, \mathrm{d}s \tag{8}$$

where $H(x)$ is the Heavyside function.

(c) The maximum value of concentration on the section S

$$c_\mathrm{m} = \max_S \{c(r, \theta, z = nL_0)\} \tag{9}$$

4.2. Results

The numerical method used to solve the advection–diffusion equation in this section is a finite volume method using free conditions for the outlet boundary and the quadratic scheme "Quick" recommended by Hayase et al. [18] and used before by Saatdjian and Leprevost [19] for the confocal ellipses case. The grid has 240,000 elements and was tested for Péclet numbers up to 500.000.

In these numerical simulation, the dye ($c = 1$) is injected on a centred disk ($r \leqslant 0.25$), with a velocity equal to the local velocity of the axial flow.

The chaotic behaviour and the mixing properties of the flow are described by the iso-concentration surfaces (Fig. 5). The evolution of the concentration with the position $z = nL_0$ of the surface S is given by Fig. 6. When n increases, the concentration field is rapidly homogenized and shows an exponential decay for μ (a completely homogeneous field would give: $\bar{c} = c_\mathrm{m} = 0.118$, $\mu = 0$ and $S_c = 1$) and from $n = 4$, the chaotic flow gives $\mu \leqslant 0.001$.

It should be noted that the three measurements (S_c, c_m, μ) give consistent results.

When the section S corresponds to $n = 4$, the competition between advection and diffusion can be described and quantified (Fig. 7). The results for the smooth flow strongly depend on the place of the dye injection, Fig. 8 corresponding to a dye injection near the centre of one of the basic flow vortices.

4.3. Conclusion

In the limit of small Péclet number values, the diffusion phenomenon drives the mixing process. When the Péclet number is high enough, the advection plays the main role. However, if the location of the dye injection is centred, the mixture obtained with the chaotic flow ($\varphi \neq 0$) is not significantly different from that obtained with the smooth flow ($\varphi = 0$). In the limit of high Péclet numbers, the chaotic flow is more efficient. While the

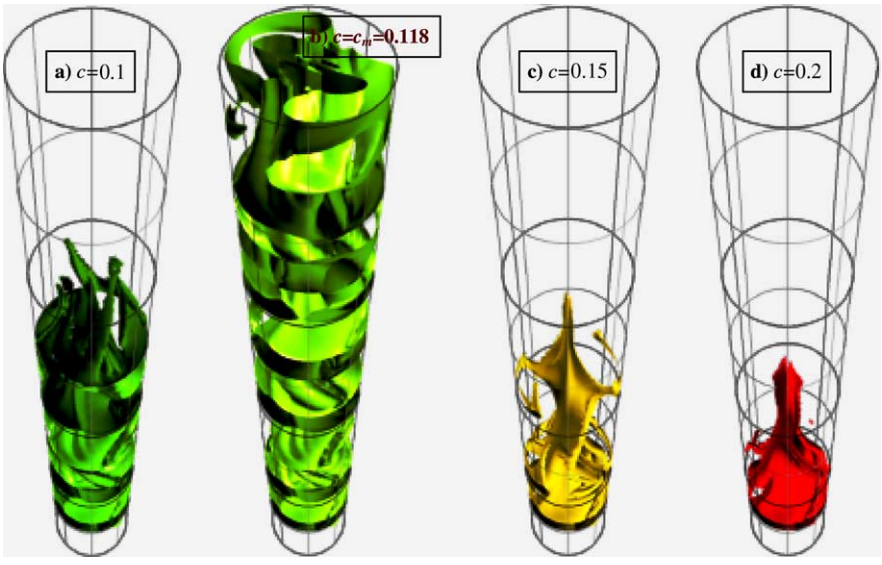

Fig. 5. Iso-concentration surfaces.

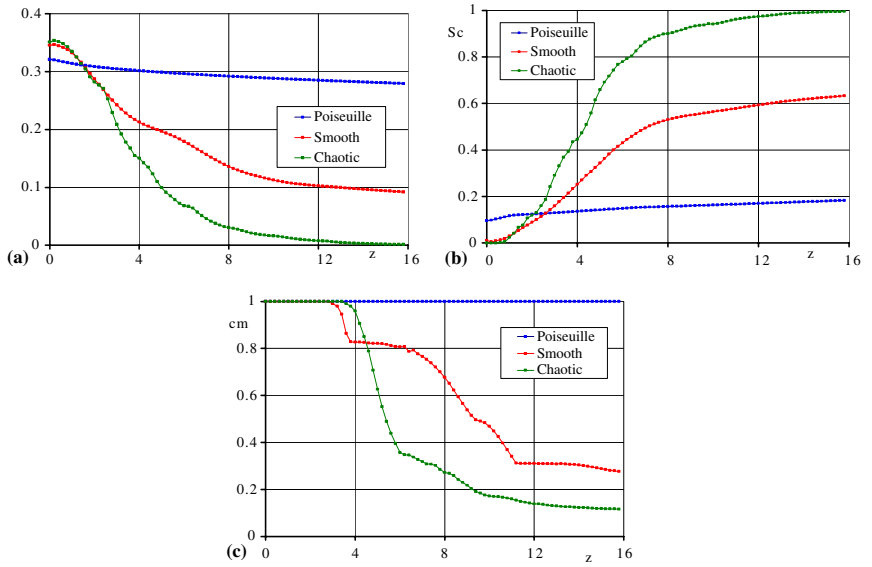

Fig. 6. (a) The mean square concentration m versus z. (b) The contaminated surface ratio S_c versus z. (c) The maximum of concentration c_m versus z (for $Pe = 50{,}000$).

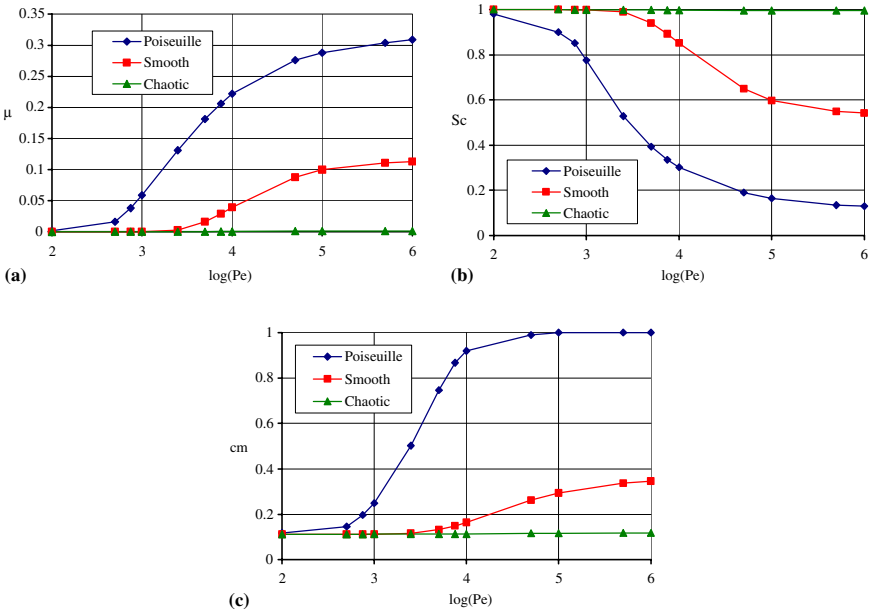

Fig. 7. Mixing properties of a centred dye injection. (a) The mean square concentration μ versus Pe. (b) The contaminated surface ratio S_c versus Pe. (c) The maximum of concentration c_m versus Pe.

mean square concentration is always close to zero for the chaotic flow, the smooth flow gives non-negligible values when the diffusion does not act.

In the case of the smooth flow, the ideal location for a dye injection is situated at the centre of the entrance section. When the dye is injected at a different position at the entrance, the mixing efficiency of the smooth flow decreases. The chaotic flow's efficiency is not affected by this modification, and the fluid seems to forget the entrance initial conditions.

The chaotic mixing process studied here is very efficient since the mixing zone covers the whole

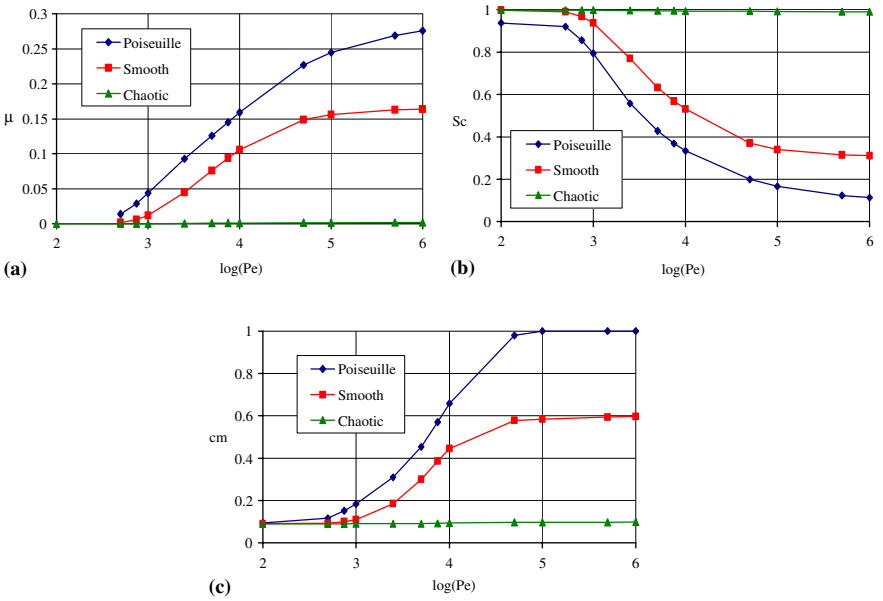

Fig. 8. Mixing properties of an eccentric dye injection. (a) The mean square concentration μ versus Pe. (b) The contaminated surface ratio S_c versus Pe. (c) The maximum of concentration c_m versus Pe.

cross-section, in contrast with eccentric cylinders or confocal ellipses processes.

Future work concerns the comparison between the temporal evolution problem in bounded flows and the spatial evolution behaviour in open flows. In particular, the decay of the mean square flux concentration with z will be carefully examined and compared with the results given in [16] concerning the temporal decay in bounded flows. If the results for a Péclet number of 50.000 (Fig. 7a) show an exponential decay, the decay-time dependence on the Péclet number and the sensibility to the entrance condition remains to be studied. Another analysis will be done. It concerns the comparison between the contaminated surface ratio and the coverage fraction of the set of intersection points of the trajectories with the outlet section. The coverage fraction defined in [7] is the ratio between the minimum number of boxes of given size required to cover this set and the section.

Appendix A

We consider the problem of a flow created in a conducting fluid by a high frequency magnetic field. The fluid is placed in a cylinder and the currents flow through two coils parallel to the axis. The frequency is sufficiently high so that the thickness of the skin layer is negligible.

When the electromagnetic forces act in a very thin skin layer, we can calculate the induced flow and by a matched asymptotic expansion we can give cinematic conditions to use on the boundary:

$$V_p(\theta) = \frac{\delta_e^2 \mu_0 I^2}{2\mu\pi^2} \frac{L^2 - 2R_0^2}{R_0} \sin(2\theta) \times \frac{2R_0^2\cos(2\theta) + L^2 + 4R_0^2}{[L^2 - 2R_0^2\cos(2\theta)]^3} \quad (A.1)$$

where I is the current through the coils, μ_0 the vacuum permeability

$$L^2 = l_0^2 + \frac{R_0^4}{l_0^2}$$

l_0 is the distance of the coils to the axis $\delta_e = \sqrt{\frac{1}{\mu_0\sigma\omega}}$, σ is the electrical conductivity, and ω is the pulsation of the currents.

The Stokes flow is calculated by using the stream function ψ:

$\Delta^2\psi = 0 \quad \text{if } r < R_0$

with boundary conditions at $r = R_0$: $\begin{cases} \psi = 0 \\ \frac{\partial\psi}{\partial n} = -V_p \end{cases}$.

The analytical solution has the following expression:

$$\psi(r,\theta) = A\left(1 - \left(\frac{r}{R_0}\right)^2\right) \sum_1^\infty g_n(d) \left(\frac{r}{R_0}\right)^{2n} \sin(2n\theta) \quad (A.2)$$

where

$$A = \frac{\mu_0 I^2}{2\mu\pi^3} \left(\frac{\delta_e}{R_0}\right)^2 \left(d - \frac{1}{d}\right)^2 \quad (A.3)$$

and

$$g_n(d) = \int_0^{\pi} \frac{2\cos(2\theta) + (d^2 + 1/d^2) + 4}{\left[(d^2 + 1/d^2) - 2\cos(2\theta)\right]^3} \times \sin(2\theta)\sin(2n\theta)\,\mathrm{d}\theta, \quad \text{with } l_0 = d \cdot R_0 \ (d > 1) \tag{A.4}$$

These results can be found in [6] and the theory of skin dynamics giving the boundary condition on the velocity in [17].

References

[1] P.D. Swanson, J.M. Ottino, A comparative computational and experimental study of chaotic mixing of viscous fluids, JFM 213 (1990) 227–249.

[2] T. Kaper, S. Wiggins, An analytical study of transport in Stokes flows exhibiting large-scale chaos in the eccentric journal bearing, JFM 253 (1993) 211–243.

[3] J. Chaiken et al., An analytical study of transport in Stokes flows exhibiting large-scale chaos in the eccentric journal bearing, Proc. R. Soc. London, Ser. A 408 (1986) 165–174.

[4] H. Aref, Chaotic advection in a Stokes flow, Phys. Fluids 29 (1986) 3515–3521.

[5] E. Saatdjian et al., Chaotic mixing and heat transfer between confocal ellipses: experimental and numerical results, Phys. Fluids 8 (1996) 677–691.

[6] J.P. Brancher, S. Goichot, Etude d'un procédé de brassage électromagnétique en écoulement de Stokes, CRAS serie II G 327 (1999) 745–751.

[7] J.C. Leprevost, J.R. Angilella, J.P. Brancher, Geometrical analysis of chaotic mixing in a low Reynolds number MHD quadripolar flow, Phys. Rev. E 63 (2001) 1–9, 056309.

[8] H.A. Kusch, J.M. Ottino, Experiments on mixing in continuous chaotic flows, JFM 236 (1992) 319–348.

[9] J.C. Leprevost, Thesis INPL, Nancy, 2000.

[10] Dombre et al., Chaotic streamlines in the ABC flows, JFM 167 (1986) 353–391.

[11] K. Bajer, H.K. Moffatt, On the effect of a central vortex on a stretched magnetic flux tube, JFM 212 (1990) 337–363.

[12] V. Toussaint, P. Carrière, F. Raynal, A numerical Eulerian approach to mixing by chaotic advection, Phys. Fluids 7 (1995) 2587–2600.

[13] S.W. Jones, O.M. Thomas, H. Aref, Chaotic advection by laminar flow in a twisted pipe, JFM 209 (1989) 335–357.

[14] A. Mokrani, C. Castelain, H. Peerhossaini, The effects of chaotic advection on heat transfer, Int. J. Heat Mass Transfer 40 (1997) 3089–3104.

[15] F. Raynal, Thesis University, Lyon I, 1994.

[16] V. Toussaint et al., Spectral decay of a passive scalar in chaotic mixing, Phys. Fluids 12 (2000) 2834–2844.

[17] H.K, Moffatt, High frequency excitation of liquid metal systems, Symposium IUTAM, Metallurgical Applications of MHD, 1982, pp. 180–189.

[18] T. Hayase, J.A.C. Humphrey, R. Greif, A consistently formulated QUICK scheme for fast and stable convergence using finite-volume iterative calculation procedures, J. Comput. Phys. 98 (1992) 108–118.

[19] H.A. Stone, A. Nadim, S.H. Strogatz, Chaotic streamlines inside drops immersed in steady Stokes flows, JFM 232 (1991) 629–646.